

High temperature elasticity measurements on oxides by Brillouin spectroscopy with resistive and IR laser heating

Stanislav V. Sinogeikin^{a,*}, Dmitry L. Lakshtanov^a, Jason D. Nicholas^{a,b,1},
Jennifer M. Jackson^a, Jay D. Bass^{a,b}

^a Department of Geology, University of Illinois, 245 HNB 1301 W Green St., Urbana, IL 61801, USA

^b Department of Materials Science, University of Illinois, 245 HNB 1304 W Green St., Urbana, IL 61801, USA

Available online 5 February 2005

Abstract

Knowledge of single crystal and aggregate elastic moduli of materials at high temperature is important in the development of high-temperature structural ceramics as well as for other areas of material sciences. Sound velocities, and hence elastic moduli, can be readily measured on micro-crystals, polycrystalline aggregates and amorphous materials using Brillouin scattering. We have developed techniques for determining the elastic moduli at high temperatures, using both electric resistive heating (to 1800 K) and CO₂ laser heating (to $T > 2500$ K). The full set of elastic constants of transparent oxides at high temperatures can be measured on samples with dimensions of $100 \times 100 \times 20 \mu\text{m}$ or even smaller. Compact resistance heaters of our design were used to study the temperature dependence of the elastic moduli of a variety of crystalline oxides and glasses, and can be used to observe high-temperature phase transitions involving elastic softening. The combination of Brillouin scattering with CO₂ laser heating allows measurements of the elastic moduli of oxides at even higher temperatures, approaching the melting points of refractory materials. The acoustic velocities of single-crystal MgO were measured to a maximum temperature exceeding 2500 ± 100 K. Both Brillouin and Raman measurements were performed on CO₂ laser-heated samples of single-crystal $\alpha\text{-Al}_2\text{O}_3$ to temperatures exceeding 2000 ± 100 K. Our results show that Brillouin scattering coupled with CO₂ laser heating is a viable means of performing sound velocity measurements at temperatures significantly higher than those readily made using resistance heating.

© 2005 Published by Elsevier Ltd.

Keywords: Spectroscopy; Mechanical properties; High-temperature elasticity measurements by Brillouin scattering

1. Introduction

Knowledge of the high-temperature elastic properties is fundamental for understanding the mechanical behavior and performance of structural ceramics under high temperature conditions. In particular, it is highly desirable to understand how properties such as elastic stiffness, fracture toughness, and anisotropy in mechanical behavior of composite materials depend upon the single-crystal elastic properties of the individual constituents. Such information would be extremely valuable in the design and development of high tem-

perature composites with superior properties.¹¹ In addition, the temperature derivatives of elastic moduli allow dimensional changes and stresses due to heating under physical constraints, as well as acoustic excitations to be calculated.²

Brillouin scattering provides a means of studying the high-temperature elastic properties of oxides and other refractory materials. It is an optical spectroscopy method that does not require any mechanical contact with the sample, and can be performed on very small samples with dimensions comparable to the size of a focused laser beam. From Brillouin experiments one can easily obtain the entire single-crystal elastic modulus tensor, C_{ijkl} (or C_{ij} in the reduced Voigt notation) for materials of arbitrary symmetry, and from this the aggregate elastic moduli (such as the bulk modulus, Young's modulus, Poisson's ratio, etc.) can be calculated via suitable averaging schemes. Brillouin spectroscopy can be used to study

* Corresponding author. Tel.: +1 217 333 6379; fax: +1 217 244 4996.

E-mail address: sinogeik@uiuc.edu (S.V. Sinogeikin).

¹ Present address: Lawrence Berkeley National Laboratory, 1 Cyclotron Rd, MS 62-203, Berkeley, CA 94720, USA.

other properties at high-temperature such as the refractive index,^{3,4} photoelastic properties,⁵ hypersonic attenuation,⁶ and the mechanisms of phase transitions.^{4,6–12}

The considerable potential of the Brillouin scattering technique for characterizing material properties at high temperatures has only begun to be exploited. Of the relatively few high-temperature Brillouin scattering experiments reported in the literature, most have used large samples with dimensions that typically exceed several millimeters. Although this does not present a problem for work with common materials, many novel materials of interest cannot be synthesized as large single crystals. Therefore, one emphasis in our laboratory program has been to employ methods that are suitable for experiments on microscopic-sized single crystals, and to extend Brillouin scattering studies to polycrystalline samples. Measuring the elastic properties on such samples by more conventional methods such as ultrasonic interferometry is often problematic or not possible, especially for single-crystal samples of low crystallographic symmetry.

In this paper we review both resistance and laser-heating methods developed in our laboratory that allow measurements of the full elastic modulus tensor on small samples ($\leq 100 \mu\text{m}$) to extremely high temperatures, approaching the melting points of refractory materials. We further describe the advantages and limitations of each heating method.

2. Brillouin scattering

Brillouin scattering arises from the inelastic scattering of incident light (photons) from thermally generated acoustic phonons in the sample. The Brillouin portion of the light scattered by the sample is shifted in frequency with respect to the incident light by a factor that is proportional to the velocity of the acoustic waves:

$$V = \left(\frac{\Delta\omega}{\omega} \right) \left(\frac{c}{2n \sin(\theta/2)} \right) = \frac{\Delta\omega\lambda}{2n \sin(\theta/2)} \quad (1)$$

where V is the velocity of an acoustic wave, $\Delta\omega$ is frequency shift of scattered light, ω is the frequency and λ is the wavelength of the incident light, c is the speed of light in vacuum, n is the index of refraction of the sample, and θ is the scattering angle, or the angle between the incident laser ray and scattered ray inside the sample.

Among the advantages of this technique are that it requires only very small samples, and that acoustic velocities can be measured along numerous crystallographic directions in a single sample, which makes it highly suitable for measurements on low-symmetry crystals. Brillouin spectroscopy also has several noteworthy characteristics for high-temperature measurements. First, the intensity of the Brillouin peaks increases with sample temperature.¹³ Second, no physical contact with the sample is needed, thus reducing sample contamination problems and allowing measurements on reactive samples in a controlled atmosphere. Moreover, the fact that one only needs optical access to the sample allows great flex-

ibility in furnace design. Third, for transparent oxide crystals the thermal emissivities are generally extremely low (orders of magnitude lower than those of metals),¹⁴ which results in a low background from thermal emission and allows measurements to be performed at temperatures exceeding 2000 K.^{3,15}

It can be seen from Eq. (1) that Brillouin scattering is geometry-sensitive. The scattering angle, and phonon direction must be carefully controlled in any experiment. In general, one must know the orientation of the sample crystallographic axes, crystal faces, and optical indicatrix to determine the acoustic velocity and corresponding phonon direction. For practical purposes it is more convenient to use a special symmetrical geometry¹⁶ in which a plate-like sample with two flat parallel faces is oriented symmetrically with respect to the incident and scattered light directions (Fig. 1). In this geometry the phonon direction, q , is in the plane of the sample. As seen in Fig. 1, for the case of an optically isotropic material, Snell's law allows the replacement of $n \sin(\theta/2)$ with $n_0 \sin(\theta^*/2)$ in Eq. (1), where θ^* is the predefined external scattering angle, and n_0 is the refractive index of air, which for practical purposes is set equal to 1. The main advantage of this "platelet symmetric geometry" is that velocities are measured independent of the sample refractive index, (which changes appreciably with temperature, pressure, and across phase transitions) so long as two principal axes of the optical indicatrix are within the plane of the platelet (a condition that is usually easy to satisfy). This geometry is especially advantageous when the sample is mounted inside a high-pressure diamond anvil cell, or a high-temperature cell.

Another geometry commonly used in high-temperature experiments is back-scattering (BS) geometry.^{3,17} In this geometry the incident laser light is focused and the scattered light is collected through the same lens ($\theta = \theta^* = 180^\circ$), and the sampling phonon direction is identical to the direction of the incident/scattered light inside the sample. Because BS geometry requires optical access in only one direction, it places

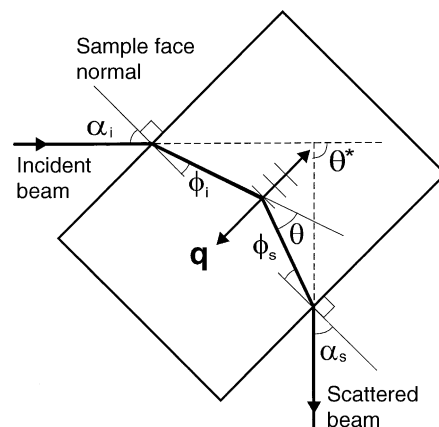


Fig. 1. Platelet, or symmetric, scattering geometry. Solid lines indicate directions of the incident and scattered beams in the sample (rectangle). α and ϕ are the angles between the incident (i) and scattered (s) beams and sample face normals. q is the phonon direction. θ is the actual scattering angle, and θ^* is the external scattering angle.

minimal restrictions on the design of high-temperature cells. In general, heaters designed to be used with Brillouin scattering in a BS geometry can achieve higher temperatures with better thermal stability (lower temperature gradients). The major disadvantages of BS geometry is that normally only longitudinal acoustic modes are observed, and that the measured Brillouin shift is proportional to the product of the acoustic velocity and the refractive index ($\Delta\omega = 2nV/\lambda$). Although obtaining single crystal elastic moduli is somewhat problematic with BS geometry, it has proved useful in studies of phase transitions.¹² Also, the combination of platelet and back-scattering geometry can provide information on the refractive index of the sample.^{3,17}

The velocities of acoustic phonons are related to the adiabatic elastic moduli and density of a material through Christoffel's equation:¹⁸

$$|C_{ijkl}q_jq_l - \rho V^2\delta_{ik}| = 0 \quad (2)$$

where V is phonon velocity, q_j and q_l are unit vectors in the phonon propagation direction, C_{ijkl} is the elasticity tensor for the material, ρ is the density, and δ_{ik} is the Kröner delta function. Using Eq. (2), the measured acoustic velocities in known crystallographic directions can be inverted to obtain the single crystal elastic moduli using, for example, a linearized general least-squares inversion procedure.¹⁹

The minimum number of crystallographic directions in which the velocities need to be measured to obtain the complete elasticity tensor depends on the crystal class. Lower symmetry materials have more independent single-crystal elastic moduli.²⁰ For example, cubic materials (e.g., MgO, YAG) are characterized by three independent elastic moduli and require measurements of longitudinal and transverse acoustic velocities in two distinct crystallographic directions, whereas orthorhombic crystals with nine single-crystal elastic moduli generally require velocity measurements in six directions.

3. Brillouin system

Descriptions of the instrumentation used in our Brillouin measurements are given in Ref. 21. A schematic diagram of the Brillouin system currently in use is shown in Fig. 2. Briefly, light from an Ar-ion laser ($\lambda = 514.5$ nm) passes through a polarization rotator and Glan-Thompson polarizer in series, which allows control of both the polarization and intensity of the incident light. Samples are typically mounted on an Eulerian Cradle so that their orientation can be varied and phonon directions probed over a wide angular range. The incidence angle is typically 40° or 45° (80° – 90° platelet symmetric scattering geometry). The light is focused on the sample with a lens with focal distance of 25–50 mm, and the scattered light is collected by a small f -number (~ 3.4) lens. A vertical aperture mask in front of the collection lens minimizes astigmatism caused by the windows in high tem-

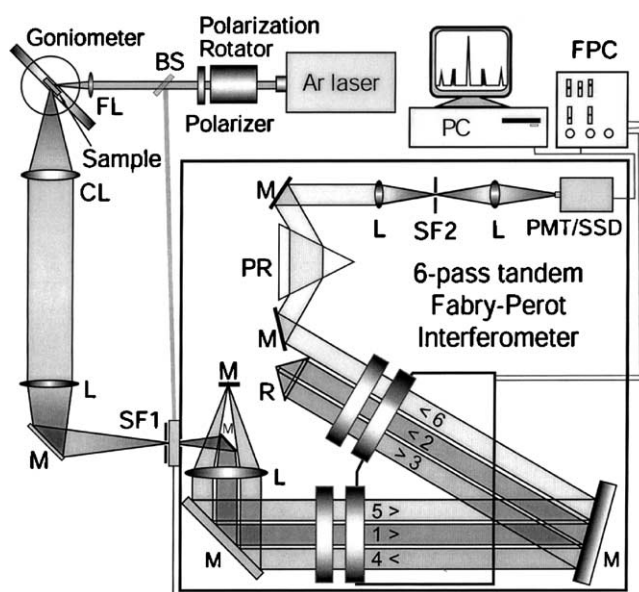


Fig. 2. Schematic diagram of the Brillouin spectrometer with six-pass Fabry-Perot interferometer. Abbreviations: BS, beam splitter; FL, focusing lens; CL, collecting lens; L, lens; M, mirror; SF, spatial filter; R, retroreflector; PR, prism; PMT/SSD, photomultiplier tube or solid-state detector; FPC, Fabry-Perot interferometer control unit.

perature cells, and increases the sharpness of Brillouin peaks. The scattered light is directed to either a Raman spectrometer, or to a piezoelectrically scanned plane-parallel tandem Fabry-Perot interferometer,¹³ used in six-pass configuration. The tandem interferometer suppresses neighboring orders of scattered light. A combination of a dispersing prism and a spatial filter after the Fabry-Perot interferometer serves as an interference filter, removing any fluorescence and most of the thermal radiation generated by the sample so that it does not show as a high background in Brillouin spectra.

4. Resistance heating

4.1. High-temperature cells

4.1.1. Symmetric (Brillouin) high-temperature cell

We have designed a high-temperature cell for use with symmetric scattering geometry Brillouin experiments (Figs. 3 and 4) to temperatures in excess of 1500 K.²² The cell is compact (about 5 cm in maximum dimension), and easily fits onto a standard three- or four-circle goniometer, allowing a number of additional applications such as X-ray scattering. Because the cell mounts on a goniometer, one obtains very good control of the scattering geometry, and any phonon direction within a plane of the platelet can be easily sampled by changing the χ -angle of the goniometer. Finally, the cell is easily used with very small samples (e.g., $100 \times 100 \times 20 \mu\text{m}$ or smaller).^{23–25}

The main body of the original cell can be constructed from a machinable alumina silicate ceramic²² or metal (Inconel) depending on temperature requirements. A metal cell pro-

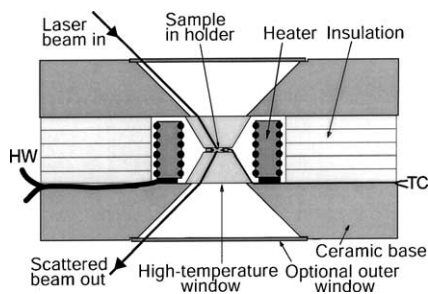


Fig. 3. Schematic diagram of Brillouin scattering in the high-temperature symmetric Brillouin cell. TC: thermocouples, HW: heating wires.

vides better mechanical stability and is easier to handle, but the high thermal conductivity of the metal body limits the maximum temperature to about 1300–1400 K if a Pt–Rh heating element is used. With a ceramic symmetric cell up to this point we were able to achieve temperatures exceeding 1600 K.

For windows we used a variety of refractory transparent materials. Fused silica windows are adequate to 1500 K, but can lose optical quality or soften at higher temperatures. Silica can also react with other cell materials, such as high-temperature cements, at high temperature. As alternative window materials we have used single-crystal sapphire and cubic zirconia, both of which have higher temperature stability and lower chemical reactivity. The disadvantage of these windows is that their higher refractive indices introduce more astigmatism that diminishes the quality of the Brillouin peaks and increases collection times. As a heating element we typically use Platinum or Platinum₇₀Rhodium₃₀ wire, wound on both sides of a threaded ceramic core. We use the largest pos-

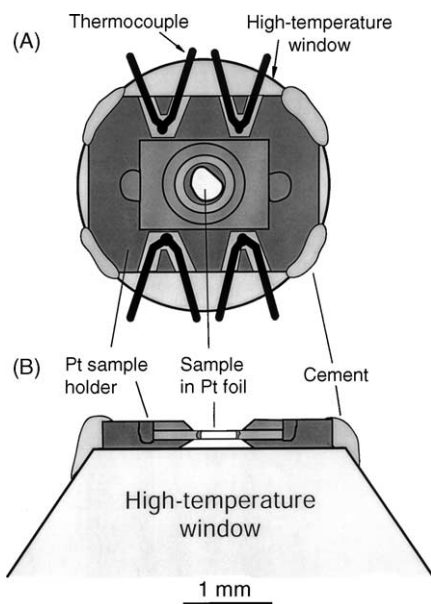


Fig. 4. Top-view (A) and cross-section (B) of sample mounting on a window. This setup shows a small sample embedded into platinum foil and polished plane-parallel together with the foil. If a sample is large enough ($>300\ \mu\text{m}$) it can be inserted into platinum holder without using the foil.

sible ratio of heater length-to-inner diameter of the heater to minimize temperature gradients. It was found that the double-coil design of the heater (the heating wire wound inside and outside of the heater core) produces more stable temperatures and smaller temperature gradients in the sample chamber.

The temperature is measured directly by two or more thermocouples (K or R type) through a computer data acquisition board. The thermocouples are attached with high-temperature cement to a window or embedded into a platinum sample holder (Fig. 4).^{23,26} The thermal mass of a relatively large Pt sample holder helps to damp out any temperature fluctuations in the cell. At the highest temperatures, the temperature fluctuations usually do not exceed 2° over several hours of operation.

Samples can be cemented directly onto the window,^{22,25} or embedded into a thin platinum foil²⁴ that is cemented to the cell window, with thermocouples placed around the sample (e.g., Fig. 5 in Ref. 22). In later experiments we used $250\ \mu\text{m}$ thick platinum foil as a sample holder to provide thermal mass. The sample is either cemented into the holder, or to avoid reaction with a cement it can be placed in a recess and held with a platinum cap (Fig. 4).

4.1.2. Axial (synchrotron) high-temperature cell

We have designed an alternative ceramic heating cell with limited optical access (Fig. 5) for backscattering Brillouin

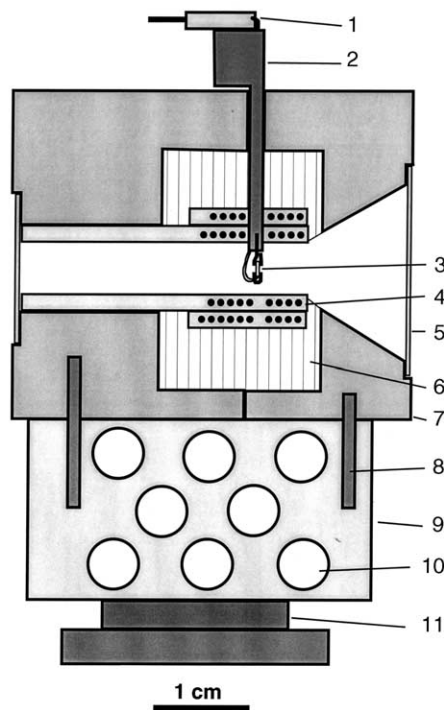


Fig. 5. High-temperature axial ceramic furnace for back-scattering Brillouin, Raman, and synchrotron X-ray measurements. (1) Thermocouple connector; (2) ceramic thermocouple/sample holder; (3) sample holder with sample and thermocouple; (4) heating elements; (5) silica glass/MgO window; (6) insulating ceramic fiber tape; (7) ceramic furnace body; (8) pins; (9) ceramic base; (10) through holes in ceramic base to minimize its thermal conductivity; and (11) metal base for mounting the furnace.

measurements or for synchrotron X-ray measurements of thermal expansion.²⁷ This cell also fits easily onto a standard X-ray goniometer and is compatible with our Brillouin system. The advantages of this cell over the cell for symmetric scattering experiments are higher thermal stability, lower thermal gradients (due to the aspect ratio of the furnace and better thermal insulation), and higher temperatures (up to 1800 K with Pt₇₀Rh₃₀ heating elements).

The limited optical access provided by this cell allows it to be used only in back-scattering or near-forward scattering geometries. While such measurements do not provide acoustic velocities and elastic moduli directly without the knowledge of the refractive index, they can be extremely useful in studying phase transitions.¹² In addition to X-ray diffraction and Brillouin experiments, this cell has been used for other high-temperature applications such as measurements of the refractive index and Raman scattering.²⁸

4.2. Results using resistance heating

4.2.1. Single crystals

The symmetric high-temperature cell has been used to measure the elastic properties of single crystal MgO, which is an important ceramic and is used in a variety of applications. Because the elastic properties of MgO have been investigated in several previous studies,^{17,29,30} it also provides an excellent means of assessing the accuracy of our resistance heating techniques.

The acoustic velocities in MgO as a function of temperature and crystallographic direction were measured from room temperature to 1510 ± 10 K with 100–200 K intervals, both on increasing and decreasing temperature.²² Up to the maximum temperature the Brillouin spectra were of superb quality with negligible thermal background (Fig. 6). At three temperatures (295 ± 1 K, 1073 ± 5 K, and 1510 ± 10 K) the data were collected in more than 10 crystallographic directions (Fig. 7) which allowed us to perform a “joint inversion” for

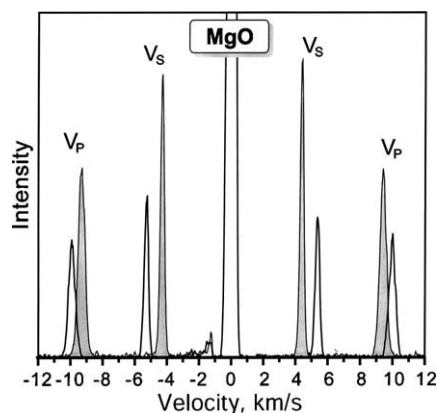


Fig. 6. Brillouin spectra of MgO in [110] direction in symmetric high-temperature cell. Unshaded peaks – room temperature spectra, shaded peaks – spectra at 1510 ± 10 K. The intensities of the peaks are scaled to fit on the same plot.

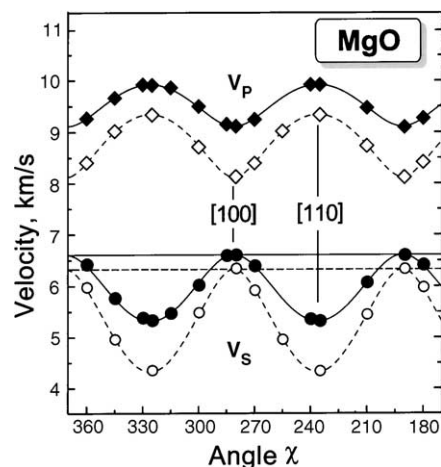


Fig. 7. Acoustic velocities in MgO as a function of crystallographic direction (χ -angle) at room temperature (solid symbols) and 1510 K (open symbols). Lines show acoustic velocities calculated from the best-fit elastic moduli at room temperature (solid) and 1510 K (dashed).

both the crystallographic orientation of the sample and single-crystal elastic moduli.³¹ The results of the joint inversions yield sample orientations at the three different temperatures (that are within one crystallographic degree), which we applied to the data at all temperatures to calculate phonon directions. At other temperatures the data were usually collected in 6–7 directions, which provides redundancy in calculation of the three independent C_{ij} 's for cubic MgO. Note that measurements in only 3–4 crystallographic directions would be sufficient to obtain orientation and elastic moduli of such cubic phases, providing that the normal to the sample plane is known. Such a dense dataset was used to assess the internal consistency of the measurements.

Acoustic velocities were inverted for the elastic moduli using a linearized inversion procedure described by Weidner and Carleton.¹⁹ The density of MgO at high-temperature was calculated from the thermal expansion data from Refs. 32, 33. The resulting single-crystal elastic moduli are shown in Fig. 8 and listed in Table 1, along with the previous ultrasonic results of Sumino et al.³⁰ and Isaak et al.²⁹ Our Brillouin results are in agreement with previous measurements, and no systematic deviations from the trend of the ultrasonic results were observed. Further descriptions of these results are given by Sinogeikin et al.²² The excellent agreement between our results and independent measurements at lower temperatures demonstrates that our experimental techniques can be used to obtain accurate high-temperature single-crystal elasticity measurements on very small crystals to temperatures in excess of 1500 K.

The symmetric high-temperature cell was used to measure the temperature dependence of the single-crystal elastic moduli to 1473 K of Yttria (Y₂O₃), which, in the form of dense polycrystalline ceramics, has been considered for use in nuclear applications and infrared optics.² We have further performed single-crystal studies on a number of geophysically important silicate minerals, including the high-pressure poly-

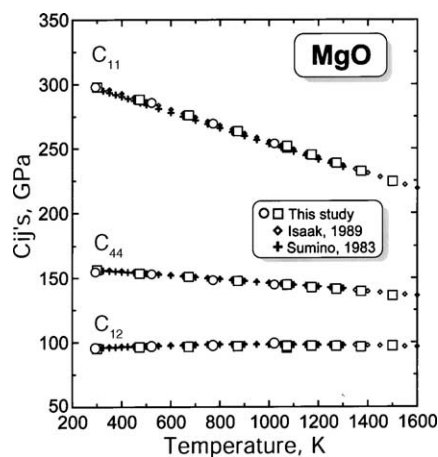


Fig. 8. Single-crystal elastic constants of MgO as a function of temperature. Open symbols (circles and squares) represent two different runs from this study. Diamonds and crosses show ultrasonic data of Isaak et al.²⁹ and Sumino et al.³⁰ for comparison. The size of the symbols is bigger than the experimental uncertainty.

morphs of olivine (γ -Mg₂SiO₄ and γ -(Mg,Fe)₂SiO₄),^{24,25} lawsonite (CaAl₂(Si₂O₇)(OH)₂·H₂O),²⁶ and magnesium-aluminum garnet—pyrope (Mg₃Al₂Si₃O₁₂).²³

4.2.2. Polycrystalline aggregates

The synthesis of crystals large enough for single-crystal elasticity measurements can be a significant experimental challenge, and the ability to measure elastic properties using polycrystalline aggregates is essential in this case. The main restriction for measurements on polycrystals is that the samples need to be well sintered, so that they are transparent and do not produce a lot of elastically scattered light. Elastic Rayleigh scattering of light from the sample generally produces a very broad central elastic peak and increases the background in these types of experiments.

Table 1
Polynomial representation of single-crystal and aggregate elastic moduli of MgO

Modulus/coefficient		This study, to 1510 K	Sumino et al. ³⁰ 300–1300 K	Isaak et al. ²⁹ 300–1600 K
C ₁₁	<i>a</i>	315.5	315.2	317.9
	<i>b</i>	−0.058	−0.062	−0.062
	<i>c</i>	−1.703	0.692	0.283
C ₄₄	<i>a</i>	158.9	160.7	161.4
	<i>b</i>	−0.010	−0.014	−0.013
	<i>c</i>	−2.773	−0.086	−1.467
C ₁₂	<i>a</i>	93.8	92.9	93.8
	<i>b</i>	0.007	0.011	0.010
	<i>c</i>	−3.084	−6.005	−5.468
K _{0s}	<i>a</i>	168.1	167.1	168.5
	<i>b</i>	−0.016	−0.013	−0.014
	<i>c</i>	−1.907	−3.616	−3.547
μ	<i>a</i>	137.7	138.6	139.6
	<i>b</i>	−0.022	−0.026	−0.025
	<i>c</i>	−1.729	0.668	−0.036

All the coefficients are given for the equation: $M(T) = a + b \times T + c \times 10^{-6} \times T^2$, where M is an elastic modulus, and T is temperature in K.

The high-temperature elastic moduli were measured on fibers of mullite ($\sim 2.5\text{Al}_2\text{O}_3 \cdot \text{SiO}_2$), a common ceramic material, to 1475 K.^{1,34} Even though the samples consisted of highly-textured polycrystalline fibers,³⁵ with crystallites having different rotation about their c axis by up to 5°, it was possible to extract all nine single crystal elastic constants (orthorhombic symmetry). That study³⁴ revealed substantial differences between bulk elastic properties calculated from “single crystal” measurements and the properties reported in the literature for polycrystalline-sintered mullite. It was shown that factors, such as microstructure, intergranular silicate glassy phases, and composition have significant effect on the elasticity of mullite ceramics, especially at high temperatures.

We also performed high-temperature elasticity measurements on a range of polycrystalline garnet-structured compounds (Mg₄Si₄O₁₂–Mg₃Al₂Si₃O₁₂ solid solutions), that are stable at high pressure and are geologically important phases in the deep Earth.²³ The measurements were performed on extremely small samples (<100 μm in lateral dimensions and $\sim 20 \mu\text{m}$ thick) with randomly oriented grains of submicron size. Such a texture allowed us to measure the aggregate acoustic velocities and elastic moduli directly, providing essential information for geophysical modeling.

4.2.3. Phase transitions

High-temperature Brillouin scattering has been extensively used to study the mechanisms of phase transitions,^{4,6–11} particularly those involving elastic mode softening. An example studied in our laboratory involves the high temperature phase transitions of enstatite (MgSiO₃),¹² an important component in some ceramics. It is well known that the low-temperature orthorhombic form of this mineral (orthoensatite) undergoes at least one phase transition to either a monoclinic (clinoensatite) or another orthorhombic nonquenchable polymorph (protoensatite). Both the temperature of this transition and the structure of the stable high temperature form are controversial.^{36,37} High temperature X-ray studies of the phase transitions in this material have not been definitive, due in part to the complexity of the crystal structures involved, the close similarities in structures of the polymorphs, the presence of twinning, and the sensitivity of the transitions to shear stresses. Our single-crystal Brillouin scattering measurements on natural orthoensatite to 1623 K at 1 atm¹² provide clear evidence for a phase transition that is accompanied by significant softening of the elastic moduli C₃₃ and C₅₅. This softening makes the occurrence of the phase transition at $1363 \pm 2 \text{ K} \leq T_{\text{Tr}} \leq 1448 \pm 7 \text{ K}$ far more obvious in the Brillouin data than in X-ray diffraction. These are the first observations of elastic softening in orthoensatite at high-temperature. The details are given in Jackson et al.¹²

4.2.4. Glass transition

A final example of the applications of resistance heating Brillouin experiments is in the glass ceramic field. The glass transformation temperature, T_g , from the glassy to the

supercooled liquid state is easily seen in Brillouin scattering measurements.^{7,15,38,39} In addition to obtaining the elastic properties by measuring the magnitude of the Brillouin shift, analysis of the widths of the Brillouin peaks gives information on relaxation and viscoelastic properties of glasses and melts. This information can in turn be related to the mobilities of atomic species in these materials.⁴⁰

5. IR laser heated measurements

Conventional high-temperature Brillouin scattering, which employs resistance heaters, can be routinely performed to temperatures of about 1500 K.^{2,12,22,34} There are a few examples of Brillouin measurements performed to higher temperatures.^{3,17} The highest temperature measurements performed by Brillouin scattering with resistive heating thus far are those by Vo-Thanh et al.¹⁵ who measured the product of the compressional acoustic velocity (V_P) and refractive index of silicate melts up to 2350 K. In theory it is possible to make resistance furnaces which will be able to achieve higher temperatures, but there are a number of limitations that make these cells impractical for Brillouin measurements.

One limitation is a high thermal background in high-temperature Brillouin spectra which, at temperatures below 2000 K, is usually related to the radiation from heater elements (e.g., heating wires and polycrystalline ceramic components), rather than a sample itself. The maximum temperature of elasticity measurements is also limited by any reactions which can take place between a sample and furnace elements or a ceramic cement, usually resulting in a deterioration of the sample at extreme temperatures.^{3,17} In addition, there are practical limitations to the construction and operation of resistance furnaces for temperatures far above 1500 K, especially for ones which are compact and have sufficient optical access for accurate Brillouin measurements. Therefore, it is desirable to use non-resistive, or contactless heating methods in order to achieve maximum temperatures and fully exploit the benefits of high-temperature Brillouin scattering.

The most effective contactless method for heating ceramic (oxide) materials is irradiation by longer-wavelength infrared lasers ($\lambda \sim 10 \mu\text{m}$). Such techniques are routinely used for thermal processing of silicates and oxides^{41,42} and material synthesis,³⁵ as well as for studying phase relations and physical properties of such materials, especially at high pressures.^{43–45} The maximum temperature which can be obtained with IR laser-heating is limited only by the maximum temperature of sample stability (melting, decomposition, deterioration) rather than heater limitations. The maximum temperature in Brillouin scattering experiments is also determined by the thermal background from the sample (which is directly proportional to emissivity of the sample). The collection of Brillouin spectra is no longer possible when the intensity of thermal emission in the region corresponding to the frequency of the laser,

exciting Brillouin scattering, is significantly higher than the intensity of Brillouin peaks, that is when Brillouin peaks can not be distinguished from thermal background. Optically transparent samples (especially well polished single crystals) have extremely low emissivity in the visible, usually orders of magnitude lower than metals. This allows relatively low thermal emission and the possibility of performing Brillouin scattering to temperatures exceeding 2000–2500 K.

5.1. Experimental methods

The CO₂ laser-heating system used with Brillouin scattering measurements is shown schematically in Fig. 9. It is based on a conventional Brillouin system (Fig. 2) with the addition of a 100 W CO₂ ($\lambda = 10.6 \mu\text{m}$) pseudo-CW laser operating in TEM₀₀ mode, a broadband spectrometer, and optical components to deliver the CO₂ laser beam to a sample and analyze Raman and incandescence spectra. The CO₂ laser is equipped with a built-in power stabilization system which provides a nominal power stability of $\pm 0.5\%$ (after warm-up). In all experiments we used an unfocused laser beam with a near-Gaussian beam profile and a full width at half maximum (FWHM) of ~ 2 mm. All Brillouin/Raman measurements were performed in a platelet symmetric scattering geometry. A detailed description of the system and experimental setup is given in Sinogeikin et al.²⁸

5.2. Results from laser-heating measurements

5.2.1. Brillouin scattering on MgO

The feasibility of performing Brillouin measurements on laser-heated samples (temperature stability, maximum

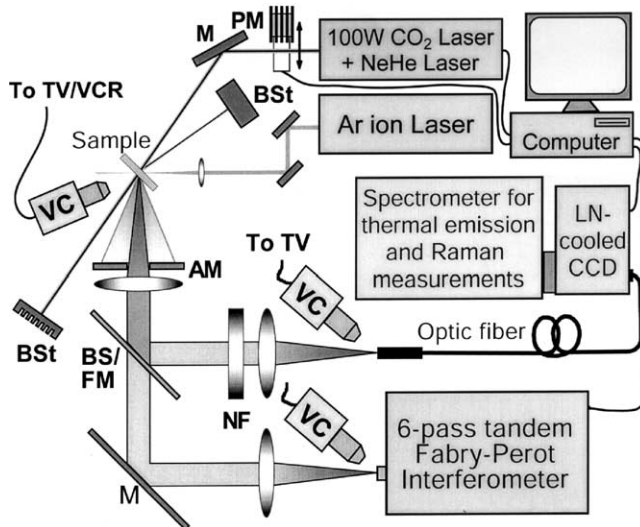


Fig. 9. Schematic diagram of the laser-heating system for Brillouin measurements. Abbreviations are: AM, aperture mask; BS, beam stop; M, mirror; BS/FM, beam splitter or flipping mirror; NF, notch filter; PM, powermeter; VC, video camera. The details of the Brillouin spectrometer are given in Fig. 3.

experimental temperatures, thermal gradients) was first demonstrated on single crystals of MgO in the (100) orientation polished plane-parallel to $\sim 50 \mu\text{m}$ thickness. The Brillouin measurements were performed in the [100] and [110] crystallographic directions. Below 1900 K the thermal background in the Brillouin spectra was negligible and became significant only above 2100 K. At high temperature the Brillouin peaks remained sharp and well defined to a temperature of ~ 2400 K (Fig. 10). At higher temperatures the quality of the spectra degraded due to an extremely high thermal background, and significantly longer collection times were necessary to obtain a reasonable signal-to-noise ratio (note that the intensity of the Brillouin peaks increases linearly with temperature,¹³ whereas the intensity of thermal radiation is proportional to T^4). Temperatures in the laser-heating experiments were obtained by comparing measured velocities of MgO with previous measurements to 1500 K with a resistance heater²² and extrapolated to higher temperatures. The acoustic velocities in this experiment served as an internal thermometer, and the temperatures calculated separately from V_P and V_S peak positions were within 80 K. We calculated that the highest temperatures of our Brillouin measurements were 2300 ± 100 K in the [100] direction and 2520 ± 100 K in the [110] direction. We believe that optimization of the system (e.g., using a shorter wavelength phonon probe, such as 488 nm) can increase the temperature limit by several hundreds of degrees.

The Brillouin measurements on laser-heated MgO were also used to access the thermal gradients in the laser-heated spot. Laser heating is a localized heating method as compared to resistive heating where the entire sample is heated uniformly. Therefore, it is important to consider axial (along the axis of CO₂ beam) and radial (perpendicular to the laser beam) temperature gradients. The radial thermal gradients

are not a serious concern in the present experiments because we used a broad unfocused CO₂ laser with FWHM ~ 2 mm, while the spectra were collected from an axial area of 40–60 μm .

The axial thermal gradients were estimated based on the width of the MgO Brillouin peaks as compared to measurements in resistively-heated cell with practically nonexistent gradients. The acoustic velocities in MgO decrease rapidly with temperature (especially $V_P^{[100]}$ and $V_S^{[110]}$)²² thus the presence of temperature gradients in a sampling volume would increase the width of Brillouin peaks. Analysis of the Brillouin peaks obtained using laser-heating indicated that the axial thermal gradients across the samples at the highest temperatures do not exceed 50 K (which is within the uncertainty of temperature determination). The further details are given in Sinogeikin et al.²⁸

5.2.2. Brillouin and Raman scattering on Al₂O₃

One of the drawbacks of laser heating (especially for transparent samples) is that the temperature cannot be measured with a thermocouple, and can only be characterized by thermal emission above 1200–1500 K in the best of cases due to extremely low emissivities of transparent oxide materials. An inability to characterize moderate sample temperatures would significantly limit the applicability of CO₂ laser heating for high-temperature elasticity measurements. Therefore, to characterize temperature in the range from ambient to 1500–2000 K, alternative ways of measuring temperature are needed.

Even though the thermal radiation is the primary way of measuring and calibrating temperatures above 1200 K,⁴⁶ there exist a variety of alternative ways of temperature measurements based on the temperature dependence of measurable physical properties of materials, for example vibrational frequencies obtained from Raman spectroscopy. Our experimental setup allows the collection of Brillouin and Raman spectra from the same spot on the sample (Fig. 9). Therefore, it is possible to use information contained in Raman spectra to characterize the temperature in the laser-heated spot (except for some cubic crystals, such as MgO, which do not produce any first-order Raman spectra). The temperature-sensitive properties of Raman spectra are anti-Stokes/Stokes intensity ratio, the widths of Raman peaks, and the absolute positions of Raman peaks.

The anti-Stokes/Stokes intensity ratio is widely used for temperature measurements.^{47–49} The theoretical limit of this method is about 1200 K, above which the anti-Stokes/Stokes intensity ratio approaches unity. In practice this method may be accurate only at temperature below ~ 750 K.⁴⁷ The widths of Raman peaks increases with temperature.^{48,50} Unfortunately, the quality (and therefore the accuracy of width measurements) of the Raman peaks progressively degrades with increasing temperature⁵¹ thereby limiting the applicability of this technique.

In our experiments as an internal thermometer, we have explored the use of temperature-induced Raman shift, which

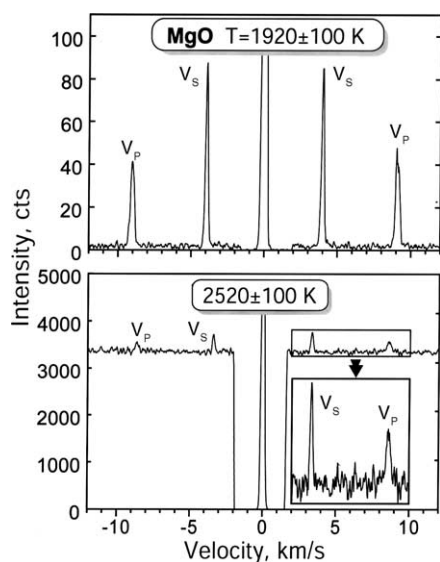


Fig. 10. Brillouin spectra of MgO in the [110] direction with CO₂ laser heating at 1920 ± 100 K and 2520 ± 100 K.

seems to be the most accurate spectroscopic method of measuring moderate temperatures.⁴⁷ The Raman shift is geometry (scattering angle) independent, and can be readily calibrated in any geometry with a variety of high-temperature devices.^{51,52}

Brillouin and Raman spectra were measured on a laser-heated sample of α -Al₂O₃ (sapphire). This material was chosen because of its importance as a ceramic, and it has been characterized by a variety of experimental techniques. Sapphire has a high melting temperature (2326 ± 3 K) and does not undergo any high-temperature phase transitions. Its single crystal elasticity at high temperature was previously measured by rectangular parallelepiped resonance to 1825 K⁵³ and by Brillouin spectroscopy to 2100 K.³

The calibration high-temperature Raman measurements were performed in an axial resistive heating furnace (Fig. 5) in a near-forward scattering geometry. An argon-ion laser ($\lambda = 514.5$ nm) was used as an excitation source. Both Stokes and anti-Stokes Raman shifts were measured to 1500 K. Above that temperature the thermal emission by the platinum holder, heater, and ceramic parts produces extremely high thermal background which significantly degraded the quality of the Raman peaks, and did not allow us to precisely determine their positions. The temperature shifts of the Raman peaks were fitted by quadratic functions.⁴⁸ The sharp and intense peak at 417 cm^{-1} gave the most consistent positions (Fig. 11). The temperatures, as calculated from the position of this peak and a fitted function in the interval from 300 to 1400 K, were within 10 K of temperatures measured by thermocouples.

The laser-heating Brillouin measurements were performed in a 80° symmetric platelet geometry on single crystals cut into $\sim 1\text{ mm} \times 4\text{ mm}$ slabs and polished to 50–60 μm thickness. High-temperature Brillouin spectra

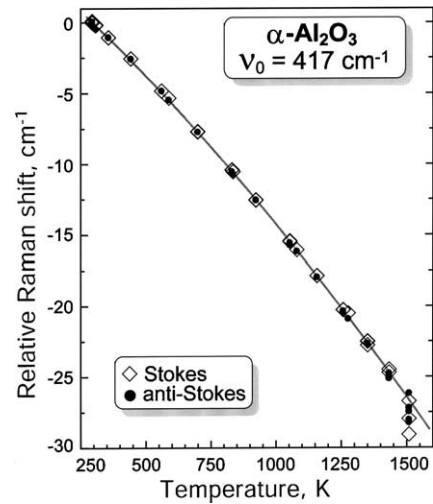


Fig. 11. Frequency shift of the most intense line (417 cm^{-1}) in the Raman spectrum of sapphire as a function of temperature measured by thermocouples in an externally—heated cell. The solid line is the quadratic least-squares best fit ($\Delta\nu = 4.95 - 0.0157 \times T - 3.4556 \times 10^{-6} \times T^2$). Data above 1400 K were not used in the fit. The uncertainty in temperature and peak positions is smaller than the size of the symbols.

were collected in the [100] and [010] crystallographic directions up to 2000 ± 100 K. Up to the highest temperature, the quality of Brillouin spectra was excellent. The thermal background in Brillouin spectra was observed only above 1900 K, but remained negligible up to the maximum temperature. Raman spectra were collected during each run before and after the Brillouin measurement and were further used to calculate sample temperature (note that the Raman and Brillouin spectra were collected from exactly the same volumes of the sample, where the light from Argon ion laser passes through the sample). Unfortunately, the Raman peaks

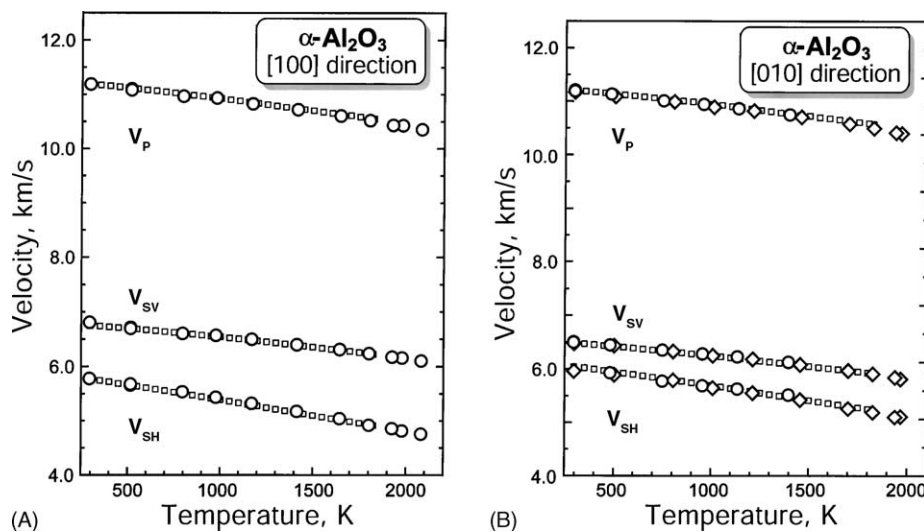


Fig. 12. Acoustic velocities in α -Al₂O₃, measured on laser-heated samples, as a function of temperature in *a*-direction ([100]) (plate A) and *b*-direction ([010]) (plate B). Diamonds and circles are measurements from this study. The temperature was calculated from the temperature-induced frequency shift of the 417 cm^{-1} Raman peak (see Fig. 11). Open squares—ultrasonic (RPR) measurements of Goto et al.⁵³

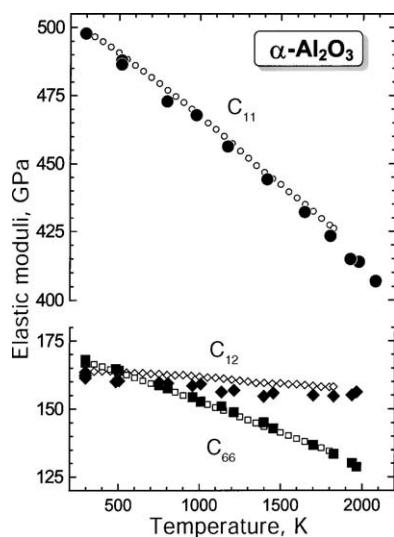


Fig. 13. Selected single-crystal elastic moduli of α - Al_2O_3 , measured on laser-heated samples, as a function of temperature (solid symbols). Open symbols are from ultrasonic measurements of Goto et al.⁵³.

were not distinguishable from the thermal background above 2000 K, which prevented us from performing measurements at higher temperatures.

The measured acoustic velocities in the [1 0 0] direction as a function of calculated temperature are shown in Fig. 12A. Fig. 12B shows the velocities measured in two distinct orientations corresponding to the [0 1 0] crystallographic direction. Also shown are the velocities calculated from single-crystal elastic moduli reported in Goto et al.⁵³ (Fig. 12A and B, open squares). From our measured velocities the single crystal moduli C_{11} , C_{66} and C_{12} were calculated (Fig. 13 and Table 2) using the thermal expansion data of Goto et al.⁵³

Table 2
Selected single-crystal elastic moduli of Al_2O_3 at high temperatures

T (K)	C_{11} (GPa)	T (K)	C_{66} (GPa)	C_{12} (GPa)
297	498	296.9	167.5	162.5
518	488	296.9	167.0	163.5
518	486	503	164.0	160.3
798	473	805.2	157.5	159.4
979	468	1008.3	152.7	159.1
1173	456	1213.7	148.8	156.8
1417	444	1456.5	142.9	155.8
1648	432	1701.6	136.8	155.0
1805	423	1826.3	133.5	154.7
1980	414	1967	128.7	156.2
1928	415	1939	130.1	155.1
2083	407	296.9	168.1	161.3
		296.9	168.1	161.3
		296.9	167.7	162.1
		484	164.6	160.0
		752.2	158.6	159.7
		957.7	154.3	158.5
		1136.6	151.0	156.2
		1398	145.1	154.6

The uncertainty in temperature is <5%. Uncertainties in C_{11} and C_{66} are 1%, and uncertainty in C_{12} is 2%. C_{12} was calculated from $C_{12} = C_{11} - 2C_{66}$.

The good agreement between our results and those measured by ultrasonic techniques demonstrates the viability of using Brillouin scattering of laser-heated samples in combination with Raman spectroscopy to obtain reliable elasticity information at moderate temperatures where the application of thermoradiometry is not possible.

6. Summary

We have developed techniques for measuring the elastic moduli of ceramic materials at high temperatures, using both external heating (to 1800 K) and laser heating (to $T > 2500$ K) of samples. The full set of elastic constants of transparent oxides (even possessing low symmetry) at high temperatures can be measured on samples with dimensions of $100 \times 100 \times 20 \mu\text{m}$ or even smaller, which is not readily achieved by other techniques.

We have designed compact resistance heaters which were used to study temperature dependence of the elastic moduli of a variety of single-crystal and polycrystalline oxide materials and glasses, and were used to observe high-temperature phase transitions involving elastic softening and glass transitions in various materials.

We have combined Brillouin and Raman scattering with CO_2 laser heating. This allowed measurements of the elastic moduli of oxides performed at yet higher temperatures, approaching melting points of refractory materials. Brillouin scattering velocity measurements with CO_2 laser heating were performed on MgO to 2510 ± 100 K (the highest temperature thus far at which Brillouin scattering measurements have been made) and α - Al_2O_3 to 2000 ± 100 K. Brillouin and Raman scattering measurements were made simultaneously at high-temperatures. The sample temperatures were inferred either from independent sound velocity measurements performed with a resistance heater (MgO), or from temperature dependence of the Raman modes (Al_2O_3).

Our results show that Brillouin scattering coupled with CO_2 laser heating is a viable means of performing sound velocity measurements at temperatures significantly higher than those readily made using resistance heating. We demonstrate the viability of combining Brillouin and Raman spectroscopies on laser-heated samples for obtaining reliable velocity measurement at moderate temperatures where the application of thermoradiometry is not possible.

Acknowledgments

We thank Brit O'Neill for help in software development for resistive heating temperature measurements. This research was supported by National Science Foundation (grants EAR EAR0002021 and 0003383) and the Air Force Office of Scientific Research (grant CWR0500).

References

- Kriven, W. M., Palko, J. W., Sinogeikin, S., Bass, J. D., Sayir, A., Brunauer, G. et al., High temperature single crystal properties of mullite. *J. Eur. Ceram. Soc.*, 1999, **19**, 2529–2541.
- Palko, J. W., Kriven, W. M., Sinogeikin, S. V., Bass, J. D. and Sayir, A., Elastic constants of yttria (Y_2O_3) monocrystals to high temperatures. *J. Appl. Phys.*, 2001, **89**, 7791–7796.
- Zouboulis, E. S. and Grimsditch, M., Refractive index and elastic properties of single-crystal corundum ($\alpha-Al_2O_3$) up to 2100 K. *J. Appl. Phys.*, 1991, **70**, 772–776.
- Askarpour, V., Manghnani, M. H., Fassbender, S. and Yoneda, A., Elasticity of single-crystal $MgAl_2O_4$ spinel up to 1273 K by Brillouin spectroscopy. *Phys. Chem. Miner.*, 1993, **19**, 511–519.
- Bucaro, J. A. and Dardy, H. D., High-temperature Brillouin scattering in fused quartz. *J. Appl. Phys.*, 1974, **45**, 5324–5329.
- Pelous, J. and Vacher, R., Thermal Brillouin scattering in crystalline and fused quartz from 20 to 1000 °C. *Solid State Commun.*, 1976, **18**, 657–661.
- Masnik, J. E., Kieffer, J. and Bass, J. D., Structural relaxations in alkali silicate systems by Brillouin light scattering. *J. Am. Ceram. Soc.*, 1993, **76**, 3073–3080.
- Ngoepe, P. E. and Comins, J. D., Brillouin scattering investigations of cerium fluoride at high temperature: a diffuse superionic transition. *Phys. Rev. Lett.*, 1988, **61**, 978–981.
- Ngoepe, P. E. and Comins, J. D., Brillouin scattering investigation of the rare-earth fluorides at high temperatures. *J. Less Common Metals*, 1989, **148**, 375–380.
- Botha, P. J., Chiang, J. C. H., Comins, J. D., Mjwara, P. M. and Ngoepe, P. E., Behavior of elastic constants, refractive index, and lattice parameter of cubic zirconia at high temperatures. *J. Appl. Phys.*, 1993, **73**, 7268–7274.
- Ngoepe, P. E. and Comins, J. D., Brillouin scattering studies of stabilized zirconias at high temperature. *J. Phys. C: Solid State*, 1987, **20**, 2983–2994.
- Jackson, J. M., Sinogeikin, S. V., Carpenter, M. A. and Bass, J. D., Novel phase transition in orthoenstatite. *Am. Miner.*, 2004, **89**, 239–244.
- Sandercock, J. R., In *Light Scattering in Solids III: Recent Results*, ed. M. Cardona and G. Guntherodt. Springer-Verlag, New York, 1982, pp. 173–206.
- Mao, H. K., Shen, G., Hemley, R. J. and Duffy, T. S., In *Properties of Earth and Planetary Materials at High Pressure and Temperature*, ed. M. H. Manghnani and T. Yagi. American Geophysical Union, Washington, 1998, pp. 27–34.
- Vo-Thanh, D., Polian, A. and Richet, P., Elastic properties of silicate melts up to 2350 K from Brillouin scattering. *Geophys. Res. Lett.*, 1996, **23**, 423–426.
- Whitfield, C. H., Brody, E. M. and Bassett, W. A., Elastic moduli of NaCl by Brillouin scattering at high pressure in a diamond anvil cell. *Rev. Sci. Instrum.*, 1976, **47**, 942–947.
- Zouboulis, E. S. and Grimsditch, M., Refractive index and elastic properties of MgO up to 1900 K. *J. Geophys. Res.*, 1991, **96**, 4167–4170.
- Love, A. E. H., *A Treatise on the Mathematical Theory of Elasticity*. Dover Publications, New York, 1944.
- Weidner, D. J. and Carleton, H. R., Elasticity of coesite. *J. Geophys. Res.*, 1977, **82**, 1334–1346.
- Nye, J. F., *Physical Properties of Crystals*. Oxford University Press, New York, 1995.
- Sinogeikin, S. V., Katsura, T. and Bass, J. D., Sound velocities and elastic properties of Fe-bearing wadsleyite and ringwoodite. *J. Geophys. Res.*, 1998, **103**, 20,819–20,825.
- Sinogeikin, S. V., Jackson, J. M., O'Neill, B., Palko, J. W. and Bass, J. D., Compact high-temperature cell for Brillouin scattering measurements. *Rev. Sci. Instrum.*, 2000, **71**, 201–206.
- Sinogeikin, S. V. and Bass, J. D., Elasticity of pyrope and majorite-pyrope solid solutions to high temperatures. *Earth Planet. Sci. Lett.*, 2002, **203**, 549–555.
- Sinogeikin, S. V., Bass, J. D. and Katsura, T., Single-crystal elasticity of $\gamma-(Mg_{0.91}Fe_{0.09})_2SiO_4$ to high pressures and to high temperatures. *Geophys. Res. Lett.*, 2001, **28**, 4335–4338.
- Jackson, J. M., Sinogeikin, S. V., Bass, J. D. and Weidner, D. J., Sound velocities and elastic properties of $\gamma-Mg_2SiO_4$ to 873 K by Brillouin spectroscopy. *Am. Miner.*, 2000, **85**, 296–303.
- Schilling, F. R., Sinogeikin, S. V. and Bass, J. D., Single-crystal elastic properties of lawsonite and their variation with temperature. *Phys. Earth Planet Inter.*, 2003, **136**, 107–118.
- Jackson, J. M., Palko, J. W., Andraut, D., Sinogeikin, S. V., Lakshatanov, D. L., Wang, J. et al., Thermal expansion of natural orthoenstatite to 1473 K. *Eur. J. Miner.*, 2003, **15**, 469–473.
- Sinogeikin, S. V., Lakshtanov, D. L., Nicholas, J. D. and Bass, J. D., Sound velocity measurements on laser-heated MgO and Al_2O_3 . *Phys. Earth Planet. Inter.*, 2004, **143–144**, 575–586.
- Isaak, D. G., Anderson, O. L. and Goto, T., Measured elastic moduli of single-crystal MgO up to 1800 K. *Phys. Chem. Miner.*, 1989, **16**, 704–713.
- Sumino, Y., Anderson, O. L. and Suzuki, I., Temperature coefficients of elastic constants of single crystal MgO between 80 and 1300 K. *Phys. Chem. Miner.*, 1983, **9**, 38–47.
- Zha, C.-S., Duffy, T. S., Downs, R. T., Mao, H.-K. and Hemley, R. J., Sound velocity and elasticity of single-crystal forsterite to 16 GPa. *J. Geophys. Res.*, 1996, **101**, 17,535–17,545.
- Suzuki, I., Thermal expansion of periclase and olivine and their unharmonic properties. *J. Phys. Earth*, 1975, **23**, 145–159.
- Dubrovinsky, L. S. and Saxena, S. K., Thermal expansion of periclase (MgO) and tungsten (W) to melting temperatures. *Phys. Chem. Miner.*, 1997, **24**, 547–550.
- Palko, J. W., Sayir, A., Sinogeikin, S. V., Kriven, W. M. and Bass, J. D., Complete elastic tensor for mullite ($\sim 2.5Al_2O_3 \cdot SiO_2$) to high temperatures measured from textured fibers. *J. Am. Ceram. Soc.*, 2002, **85**, 2005–2012.
- Sayir, A. and Farmer, S. C., Directionally solidified mullite fibers. *Mater. Res. Soc. Symp. Proc.*, 1995, **365**, 11–20.
- Kriven, W. M., Possible alternative transformation tougheners to zirconia: crystallographic aspects. *J. Am. Ceram. Soc.*, 1988, **71**, 1021–1030.
- Lee, W. E. and Heuer, A. H., On the polymorphism of enstatite. *J. Am. Ceram. Soc.*, 1987, **70**, 349–360.
- Askarpour, V., Manghnani, M. H. and Richet, P., Elastic properties of diopside, anorthite, and grossular glasses and liquids: a Brillouin scattering study up to 1400 K. *J. Geophys. Res.*, 1993, **98**, 17,683–17,689.
- Schilling, F. R., Sinogeikin, S. V., Hauser, M. and Bass, J. D., Elastic properties of model basaltic melt compositions at high temperatures. *J. Geophys. Res.*, 2003, **108**(B6), 2304.
- Kieffer, J., Masnik, J. E., Reardon, B. J. and Bass, J. D., High-frequency relaxational spectroscopy in liquid borates and silicates. *J. Non-Crystal Solids*, 1995, **183**, 51–60.
- Belov, A. V., Bubnov, M. M., Gur'yanov, A. N., Devyatykh, G. G., Dianov, E. M., Prokhorov, A. M. et al., Drawing of glass-fiber waveguides using CO₂ lasers. *Sov. J. Quant. Electron.*, 1978, **8**, 1169.
- Paek, U. C. and Weaver, A. L., Formation of a spherical lens at optical fiber ends with a CO₂ laser. *Appl. Opt.*, 1975, **14**, 294–298.
- Yagi, T. and Susaki, J. I., High-pressure research: application to earth and planetary sciences. In *High-Pressure Research: Application to Earth and Planetary Sciences*, ed. Y. Syono and M. H. Manghnani. Amer. Geophys. Union, Washington, 1992, pp. 51–54.
- Andraut, D. and Fiquet, G., Synchrotron radiation and laser heating in a diamond anvil cell. *Rev. Sci. Instrum.*, 2001, **72**, 1283–1288.
- Fiquet, G., Andraut, D., Itie, J. P., Gillet, P. and Richet, P., X-ray diffraction of periclase in a laser-heated diamond-anvil cell. *Phys. Earth Planet. Inter.*, 1996, **95**, 1–17.

46. Nicholas, J. V. and White, D. R., *Traceable Temperatures: An Introduction to Temperature Measurement and Calibration*. John Wiley & Sons, New York, 2001.
47. Cui, J. B., Amtmann, K., Ristein, J. and Ley, L., Noncontact temperature measurements of diamond by Raman scattering spectroscopy. *J. Appl. Phys.*, 1998, **83**, 7929–7933.
48. Herchen, H. and Cappelli, M. A., First-order Raman spectrum of diamond at high temperatures. *Phys. Rev. B*, 1991, **43**, 11740–11744.
49. LaPlant, F., Laurence, G. and Ben-Amotz, D., Theoretical and experimental uncertainty in temperature measurement of materials by Raman spectroscopy. *Appl. Spectrosc.*, 1996, **50**, 1034–1038.
50. Schmidt, C. and Ziemann, M. A., In-situ Raman spectroscopy of quartz: a pressure sensor for hydrothermal diamond-anvil cell experiments at elevated temperatures. *Am. Miner.*, 2000, **85**, 1725–1734.
51. Richet, P., Gillet, P., Pierre, A., Bouhifd, M. A., Daniel, I. and Fiquet, G., Raman spectroscopy, X-ray diffraction, and phase relationship determinations with a versatile heating cell for measurements up to 3600 K (or 2700 K in air). *J. Appl. Phys.*, 1993, **74**, 5451–5456.
52. Zouboulis, E. S. and Grimsditch, M., Raman scattering in diamond up to 1900 K. *Phys. Rev. B*, 1991, **43**, 12490–12493.
53. Goto, T., Anderson, O. L., Ohno, I. and Yamamoto, S., Elastic constants of corundum up to 1825 K. *J. Geophys. Res.*, 1989, **94**, 7588–7602.